Max-Planck-Institut
für Meteorologie

REPORT No. 232

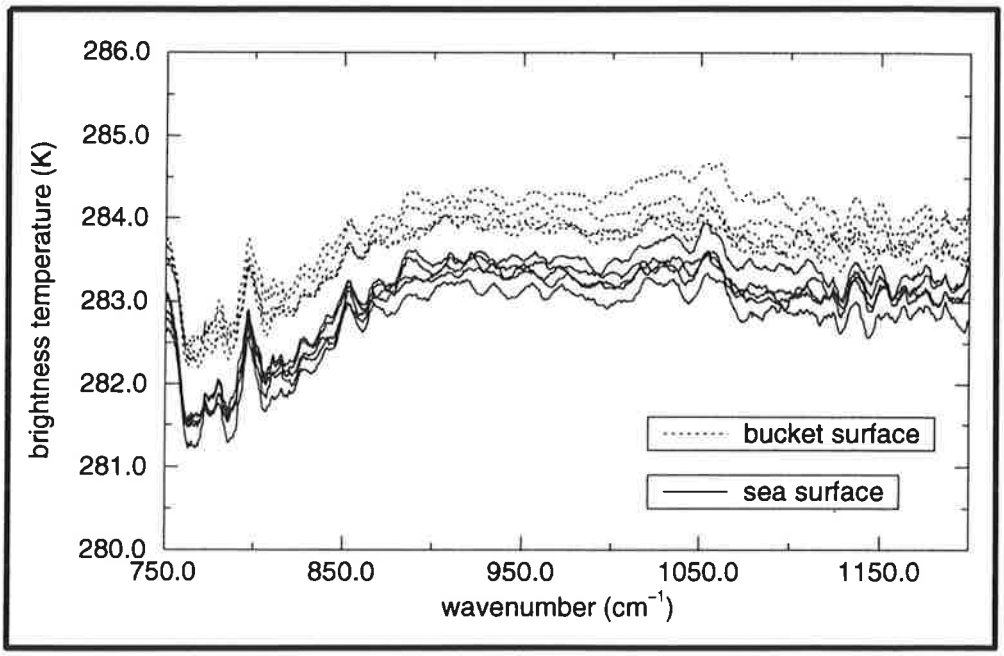

INTERFEROMETRIC MEASUREMENTS OF SEA SURFACE TEMPERATURE AND EMISSIVITY

by

Lars Fiedler · Stephan Bakan

HAMBURG, February 1997

AUTHORS:

Lars Fiedler
Stephan Bakan

Max-Planck-Institut
für Meteorologie

MAX-PLANCK-INSTITUT
FÜR METEOROLOGIE
BUNDESSTRASSE 55
D - 20146 HAMBURG
GERMANY

Tel.: +49-(0)40-4 11 73-0
Telefax: +49-(0)40-4 11 73-298
E-Mail: <name> @ dkrz.de

Interferometric measurements of sea surface temperature and emissivity

Lars Fiedler, Stephan Bakan

Max-Planck-Institut für Meteorologie,

Bundesstr. 55, D-20146 Hamburg, fiedler@dkrz.de

Abstract:

A new multispectral method to derive sea surface emissivity and temperature (SST) by using interferometer measurements of the near surface upwelling radiation in the infrared window region is presented. As reflected sky radiation adds substantial spectral variability to the otherwise spectrally smooth surface radiation an appropriate estimate of surface emissivity allows to correct the measured upwelling radiation for the reflected sky component. The remaining radiation together with the estimated surface emissivity, yields an estimate of the sea surface temperature. Measurements from an ocean pier at the Baltic Sea in October 1995 indicate an accuracy of about 0.1K for the so derived sea surface temperature. A strong sea surface skin effect of about 0.6K is found in that special case.

ISSN 0937-1060

1 Introduction

Evaporation, sensible heat flux, and longwave net radiative flux usually result in a net heat flux from the ocean surface to the atmosphere, creating the so-called cool skin of the ocean (i.e. Saunders, 1967; Graßl, 1976; Paulson and Simpson, 1981; Katsaros, 1980; Schlüssel, 1990). Due to molecular heat transfer, this cool layer extends down to a few hundred micrometers and it's temperature is found to be typically about 0.2 K less than that of the bulk water below (Schlüssel et al., 1995). The skin effect is of consequence to several climatologically relevant issues: Sea surface temperature determination from satellite data, SST parameterization in climate models, estimation and parameterization of ocean-atmosphere heat, moisture and mass fluxes (e.g. CO_2). Therefore, substantial efforts have been made in recent years to derive the skin temperature as accurately as possible and to collect examples under various circumstances for the determination of a relevant climatology (i.e. Robinson et al., 1984; Coppin et al., 1991; Schlüssel, 1995; Thomas et al., 1995; Donlon and Robinson, 1996; Smith et al., 1996).

The skin effect is usually determined from downward looking near surface radiometer measurements around 11 μm in the infrared window in comparison with bulk water temperature values. The biggest difficulty of the SST measurement with radiometers arises from the non-blackness of the sea surface, which causes reflected sky radiation to add to the surface emission. Probably the most reliable procedure to overcome this problem is to view at the surface of an intercomparison water bucket between successive ocean surface views. Sea water is constantly pumped into the bucket and discharged through a pushbroom nozzle in order to destroy the surface skin layer, so that the radiometer signal is free of the skin effect. At the same time it is assumed that the bucket surface reflects the same amount of sky radiation as the sea surface. Therefore, the radiance difference between the bucket and the sea surface view is believed to cancel the reflected sky radiation and to yield a signal proportional to the cool skin of the sea surface (Graßl and Hinzpeter, 1975; Graßl, 1976; Schlüssel et al., 1990; Schlüssel, 1995).

Other authors use radiometer measurements of the downwelling sky radiation and estimate the reflectivity of the sea surface from simultaneous measurements of the surface wind speed. The according emissivities depend on wavenumber, viewing angle, and wind speed as published by Masuda et al. (1988). This procedure has been used to calculate the SST e.g. by Barton et al. (1995), Donlon et al. (1995), Thomas et al. (1995). Coppin et al. (1991) used a similar procedure assuming a constant value for surface emissivity independent of wind speed.

In the following it is proposed to use a spectrally high resolving interferometer instead of a broadband radiometer. Such interferometers with a spectral resolution around 1 cm^{-1} are available today in rugged and field proof design at affordable cost.

Smith et al. (1996) recently applied such an interferometer instead of a radiometer on board a research vessel to infer SST and sea surface properties. They use a small spectral region around

1305 cm^{-1} centred in the emission bands of methane and nitrous oxide to estimate the SST with the help of emissivity data from Masuda et al. (1988). These SST values are in turn applied in other spectral regions for the derivation of the spectral distribution of emissivity.

In the following a somewhat different procedure for simultaneous derivation of sea surface emissivity and SST from rather highly resolved spectra is described. While the emission from the sea surface should result in a smooth spectrum, the reflected sky radiation adds spectral variability, at least in cloud free cases. The observed variability should therefore allow for the correction of reflected sky radiation. This paper describes the principle of the proposed new multispectral method (ch. 2), the available instrument, first measurements (ch. 3) and preliminary results (ch. 4).

2 Multispectral method for SST determination

The upwelling spectral radiance L_κ (κ = wavenumber) recorded by a downward pointing radiometer or interferometer consists of three contributions:

- emission from the sea surface transmitted to the interferometer (A),
- emission of the atmosphere between the sea surface and the instrument (*B*),
- the reflected part of the downwelling radiation of the atmosphere which is transmitted to the interferometer (*C*).

For an non-scattering atmosphere these contributions are described by

$$L_\kappa = \varepsilon_{\kappa,\theta,ff} B_\kappa(T_S)\exp(-\delta_\kappa^*/\mu) \qquad \text{(A)}$$

$$+ \int_0^{\delta_\kappa^*} B_\kappa(T)\exp(-(\delta_\kappa^* - \delta_\kappa)/\mu)\, d\delta_\kappa/\mu \qquad \text{(B)} \qquad (1)$$

$$+ (1-\varepsilon_{\kappa,\theta,ff})\exp(-\delta_\kappa^*/\mu) \int_0^{\delta_{\kappa,TOA}} B_\kappa(T)\exp(-\delta_\kappa/\mu)\, d\delta_\kappa/\mu \qquad \text{(C)}$$

T_S denotes the thermodynamic temperature of the sea surface, B_κ the Planck-function, $\varepsilon_{\kappa,\theta,ff}$ the emissivity of the sea surface (depending on wavenumber κ, viewing zenith angle θ, and wind speed ff), μ the cosine of the zenith angle, $\delta_{\kappa,\,TOA}$ the total optical thickness of the atmosphere, and δ_κ* the optical thickness between the sea surface and the instrument level.

To assess the emitted contribution (B) of the layer between the sea surface and the instrument, line-by-line radiative transfer calculations (Hollweg, 1989) have been carried out for the measurement situation described in Ch. 3.

Fig. 1 shows, that the contribution to the surface brightness temperature is smaller than 0.05K from 770 to 1100 cm^{-1}, due to the location of the interferometer near the sea surface. Since the contribution from the reflected sky emission (C) is in the order of 1K, (see Ch. 3) the direct emission component (B) is neglected in the following procedure. For the same reason the absorption factor in term (A) is set equal to 1.

If the reflected sky radiation would also be negligible the recorded spectrum should be spectrally smooth. This is because the emissivity $\varepsilon_{\kappa, \theta, ff}$ is a smooth function of wavenumber, observation angle and wind speed (Friedmann, 1969; Sindran, 1981; Masuda et al., 1988). The Planck-function is also a smooth function of wavenumber.

Reflected sky radiation (C), however, adds considerably to the surface emission, introducing spectral line and band characteristics to the radiation registered by the interferometer. This spectral signature can be used to correct the observed spectrum for the atmospheric reflected sky radiation component. An appropriately weighted amount of downwelling sky radiation is subtracted from upwelling radiation detected by the interferometer until the remaining spectrum becomes smooth. The weighting coefficient represents the surface reflectivity, which in turn yields the emissivity of the ocean surface. From this information the Planck-function of the sea surface can now be calculated. Consequently the sea surface temperature can be estimated by inverting the Planck-function. Not only the dominant contributions of the line and band emission from water vapour and CO_2 are accounted for, but the water vapour continuum emission is also considered (Fiedler, 1996).

The proposed procedure to derive the sea surface temperature consists of the following steps:

1. Correction for the atmospheric emission between ocean surface and the instrument, which is usually negligible for the window range 770 - 1100 cm^{-1}.
2. Correction for the reflected sky emission by subtracting a weighted part of the sky spectrum from the sea surface spectrum, until the resultant spectrum is as smooth as possible. Here, a least squares procedure is applied to spectral intervals of about 100 cm^{-1} width in order to follow the spectral variability of surface emissivity to estimate the optimum weight.
3. The derived reflectivity yields also the surface emissivity, since the transmissivity of the sea water is small in the IR window region (Schlüssel, 1995). The spectral Planck-function according to the surface temperature T_S is then derived as the ratio of the measured radiance, which is corrected for the reflected sky emission and the surface emissivity.

This procedure should also work in case of thin or high level clouds with brightness temperatures considerably smaller than that of the surface, but not for rather thick low level clouds. These clouds emit almost like a blackbody of environmental or sea surface temperature as the cloud base temperature is not far from the SST. The additional emission in the line centers of water vapour add only little to this background signal so that the spectral variability of downwelling sky radiation is small in this case. As the spectral shape is similar to that of a blackbody at sea surface temperature it is not possible to distinguish between the contributions from the sky and the sea surface in the upwelling radiation.

3 Measurements

The observation equipment for the necessary measurements is sketched in Fig. 2. Measurements have been taken from the head of an ocean pier at the Baltic sea shore near Graal-Müritz, Germany, between 19 and 23 Oct. 1995.

The equipment consisted of an interferometer, which subtended a nadir view angle of 53° towards the ocean. The interferometer is of the BOMEM MR 154 type, which uses the double pendulum principle with corner cube mirror arrangement. A liquid nitrogen cooled MCT detector for the spectral range 600 - 2000 cm^{-1} was used at a spectral resolution of 1 cm^{-1}. For the calibration, a Galai BB-50 variable temperature calibration blackbody was moved into the field of view of the interferometer at regular intervals. The calibration was performed at least every 30 minutes. The calibration source properties are given in Table 1 :

Table 1: Properties of the calibration source BB-50

parameter	value
temperature range	-20°C to 100°C
accuracy	0.1° C
diameter	5.5 cm
emissivity	0.99 ± 0.005
stabilizing-time	~ 20 minutes

Measurements at two temperatures allowed a linear calibration procedure according to Revercomb et al. (1988).

Moreover a calibration water bucket was alternately moved into the field of view of the interferometer for intercomparison purposes. This bucket is constantly flooded with sea water, which is discharged through a pushbroom type nozzle in the middle. The purpose is to destroy the surface skin layer so that no skin effect is observable. The water temperature in the bucket was monitored at a depth of about 1 cm as well as the bulk water temperature in 1.5 m depth

with platinum resistant thermometers.

In addition, a data acquisition system for standard meteorological data was operated.

Unfortunately no measurements of the downwelling atmospheric radiation were possible, due to the necessary sea spray protection. Therefore sky radiation spectra taken a few weeks earlier during an intercalibration measurement campaign at Potsdam, Germany, are applied in the following data evaluation.

The data used in this study come from a measurement phase between 0:40 and 4:30 on 22 Oct. This phase is characterized by clear sky with a net radiative flux of ~150 W/m^2, onshore wind at around 4 m/s, relative humidity of 80%, sea surface temperature of 12 °C and air temperature of 2 °C. This large temperature difference results in a total bulk heat flux of about -340 W/m^2 (calculated after Hasse, 1971).

4 Results and Discussion

Fig. 3 displays calibrated brightness temperature spectra of the sea (full lines) and the bucket surface (dotted lines). In the spectra, the reflected downwelling sky emission can be clearly identified as the ozone band at 1040 cm^{-1} and the water vapour bands at 800 cm^{-1} and 860 cm^{-1}. To smooth the displayed spectrum a weighted running average filter (Savitzky and Golay 1964) of 12 cm^{-1} halfwidth has been applied to the spectra of sea and bucket surface. The individual spectra cover a time range of 6.5 minutes each and their differences indicate the variability of the sea surface temperature. Bucket temperatures have been increased according to the measured temperature difference between the ocean bulk (at 1.5 m depth) and the bucket (1 cm below surface). Although the spectra of the bucket surface are not required for the presently proposed method, they are included for reference. As that surface should be free of a cool skin these spectra provide a test case for the procedure.

Fig. 4 shows the derived spectral reflectivity of the sea (full line) and the bucket surface (dotted line). The reflectivity is an average over 32 spectra, which are collected during 4 hours with cloud free sky. The error bars indicate the rms difference between individual calculations of reflectivity. For comparison, the theoretical values provided by Masuda et al. (1988) for 50° view angle and 3 m/s wind speed are added. Their size and spectral distribution is similar to our observed values. The derived reflectivity values of the sea and the bucket surface exhibit significant differences below 900 cm^{-1}, which may be due to the considerably different details of the sea and bucket surface structure. On the one hand the certainly different wave spectrum may be responsible for the emission difference. On the other hand the nozzle causes a small water-bulge on the calibration bucket water surface which changes the angle of incidence of emitted and reflected radiation as compared to the sea surface. The angle of incidence at the

water bucket surface is on the average changed towards smaller values, which results in higher emissivity and a lower reflectivity in comparison to the sea surface. Above 900 cm^{-1}, the difference between the measurements of the two surfaces is no longer statistically significant, although the sea surface exhibits still consistently higher values up to 1150 cm^{-1}. At the same time the theoretical value increases to higher reflectivities than the measurements do.

The resulting spectra, which are corrected for the reflected atmospheric component and for emissivity are shown in Fig. 5. The brightness temperature spectra are almost independent of wavelenght for $\kappa > 880$ cm^{-1} as they should ideally be after the correction.

The remaining spectral variability is most probably due to the use of a somewhat inappropriate atmospheric correction spectrum that has been recorded at a different time and location.

Another reason for spectral variation of the brightness temperature could be a vertical temperature gradient below water surface. As has been discussed e.g. by Kelly (1978) the transmissivity of sea water changes considerably with wavenumber in the thermal window. The radiation leaving the water in different spectral intervals is therefore related to different depths and associated temperatures. This could in principle be used to infer the vertical temperature gradient and from this the heat flux at the water surface (Timofeev, 1966; McAlister and McLeish, 1970; McKeown et al., 1995). Reasonable temperature gradients however result in very small brightness temperature differences of less than .01 K across the thermal window. As this is definitely smaller than the accuracy limits of our measurements no conclusions about heat flux at the sea-air interface can be drawn. This situation should improve with the foreseen use of the additional spectral interval between 2300 and 3000 cm^{-1} where the transmissivity of sea water differs considerably from that of the infrared window region.

The skin effect is given by the difference between the sea and the bucket surface spectra. In this case it amounts to about 0.6 K. This is considerably smaller than the ~1K difference of the original spectra (Fig. 3), which represents the result of the standard radiometric procedure. The large value of 0.6 K is consistent with the mentioned high energy flux from the sea surface due to the clear sky night conditions.

As the bucket surface should be free of the skin effect and its temperature is measured near to the surface this provides a benchmark measurement for the accuracy of the proposed method. Fig. 6 presents the comparison between the retrieved spectrally averaged bucket surface brightness temperature (averaged from 833 cm^{-1} to 1000 cm^{-1}) and the thermodynamic temperature measured at 1 cm depth. A difference of -0.12 ± 0.07 K remains between the retrieved bucket surface and the measured thermodynamic temperature. Whether this characterizes the accuracy limit of the technique is not yet clear. Under the given strong cooling conditions it may also signify that the suppression of a cool skin on the bucket surface was not complete.

5 Conclusions

These first results suggest that the proposed technique is able to provide the sea surface temperature with an accuracy of the order of 0.1 K. This is possible without additional assumptions and measurements (i.e. with a water bucket) as are required for the standard radiometric procedure. To generalize this conclusion, additional measurements have to be carried out, including simultaneously measured sky spectra.

The advantage of the new multispectral method is that the surface emissivity is estimated directly from the measurements and is not parameterized or taken from theoretical calculations to determine the SST as in former methods. The multispectral method offers the opportunity to distinguish between the change of emissivity and SST. This is not possible with a classical radiometer since both changes can result in the same brightness temperature variation due to the wide spectral range.

The direct measurement of sea surface emissivity shall be used to study properties of surface films which change sea surface emissivity. Such measurements would complement earlier studies with different techniques (Jarvis, 1962; Alpers et al., 1982). This is important since surface films play a relevant role in the interaction between ocean and atmosphere and cover up to 70% of the ocean surface (GESAMP, 1995; Schlüssel, 1995). This technique should also prove useful in future studies for remote sensing of total heat flux between ocean and atmosphere.

6 Acknowledgement

The authors are indebted to P. Schlüssel for valuable discussions, to A. Kirchgäßner for help with the measurements, to H.-H. Brecht for his technical support, to B. Zinecker for editing the manuscript, and to the community administration of Graal-Müritz for providing the measurement site.

7 References

Alpers, W., H.-J. C. Blume, W. D. Garrett, H. Hühnerfuß 1982: The effect of monomolecular films on the microwave brightness temperature of the sea surface, *Int. J. Remote Sensing*, **3**, 457-474.

Barton, I.J., A. J. Prata, and R. P. Cechet 1995: Validation of the ATSR in Australian waters, *J. Atmos. Oceanic Technol.*, **12**, 290-300.

Coppin, P. A., E. F. Bradley, I. J. Barton, J. S. Godfrey 1991: Simultaneous observations of sea surface temperature in the western equatorial pacific ocean by bulk, radiative and satellite methods, *J. Geophys. Res.*, **96**, 3401 - 3409.

Donlon, C. J., I. S. Robinson 1996: Observations of the oceanic thermal skin in the Atlantic ocean, unpublished paper.

Fiedler, L. 1996: Bestimmung des Wärmeflusses an der Grenzfläche Luft-Wasser mittels FTIR-Spektrometrie, Diplomarbeit im Fach Meteorologie, Universität Hamburg.

Friedmann, D. 1969: Infrared characteristics of ocean water (1.5 - 15 μ), *Appl. Opt.*, **8**, 2073-2078.

GESAMP (IMO/FAO/Unesco-IOC/WMO/WHO/IAEA/UN/UNEP) Joint Group of Experts on the Scientific Aspects of Marine Environmental Protection **1995:** The sea-surface and its role in global change, *Rep. Stud. GESAMP*, **59**.

Graßl, H. and H. Hinzpeter 1975: The cool skin of the ocean, *GATE Report 14*, Vol. I, WMO. Geneva, 229-236.

Graßl, H. 1976: The dependence of the measured cool skin of the ocean on wind stress and total heat flux, *Boundary-Layer Meteorol.*, **10**, 465-474.

Hasse, L. 1971: The sea surface temperature deviation and the heat flow at the sea-air interface, *Boundary-Layer Meteorol.*, **1**, 368-379.

Hollweg, H.-D., 1989: Line-by-line model for the calculation of infrared radiation fluxes and the cooling rates in clear sky atmospheres, *Max-Planck-Institut für Meteorologie, Report* No. 36.

Jarvis, N.L. 1962: The effect of monolayer films on surface temperature and convective motion at the water/air interface, *J. Colloid Sci.*, **17**, 512-522.

Katsaros, K.B. 1980: The aqueous thermal boundary layer, *Boundary-Layer Meteorol.*, **18**, 107-127.

Kelly, C. S. 1978: Effective infrared optical depths associated with the clear ocean, *Appl. Opt.* **17**, 3054-3059.

Masuda, K., T. Takashima, and Y. Takayama 1988: Emissivity of pure and sea waters for the model sea surface in the infrared window regions, *Remote Sensing of Environment*, **24**, 313-329.

McAlister, E.D. und W. McLeish 1970: A radiometric system for airborne measurement of the total heat flow from the sea, *Appl. Opt.*, **9**, 2697-2705.

McKeown, W., F. Bretherton, H.L. Huang, W.L. Smith and H.L. Revercomb, 1995: Sounding the skin of water: sensing air-water interface temperature gradients with interferometry, *J. Atmos. Oceanic Technol.*, **12**, 1313-1327.

Paulson C. A. and J.J. Simpson 1981: The temperature difference across the cool skin of the ocean, *J. Geophys. Res.*, **86**, 11044-11054.

Revercomb, H.E., H. Buijs, H.B. Howell, D.D. Laporte, W. L. Smith and L. A. Sromovsky, 1988: Radiometric calibration of IR Fourier transform spectrometers: Solution to a problem with High-Resolution Interferometer Sounder, *Appl. Opt.*, **27**, 3210-3218.

Robinson, I. S., N. C. Wells and H. Charnock 1984: The sea surface thermal boundary layer and its relevance to the measurement of sea surface temperature by airborne and spaceborne radiometers, *Int. J. Remote Sensing*, **5**, 19-45.

Saunders, P.H. 1967: The temperature at the ocean-air interface, *J. Atmos. Sci.*, **24**, 269-273.

Savitzky, A. and M.J.E. Golay 1964: Smoothing and differentiation of data by simplified least squares procedures, *Analyt. Chem.*, **36**, 1627-1639.

Schlüssel, P. 1995: Passive Fernerkundung der unteren Atmosphäre und der Meeresoberfläche aus dem Weltraum, *Berichte aus dem Zentrum für Meeres- und Klimaforschung,* Reihe A, Nr. 20.

Schlüssel, P., W.J. Emery, H. Graßl and T. Mammen 1990: On the bulk-skin difference and its impact on satellite remote sensing of the sea surface temperature, *J. Geophys. Res.*, **95**, 13341-13356.

Sidran, M. 1981: Broadband reflectance and emissivity of specular and rough water surfaces, *Appl. Opt.*, **20**, 3176-3183.

Smith, W.L., R.O. Knuteson, H.E. Revercomb, W. Feltz, H.B. Howell, W.P. Menzel, N. Nalli, O. Brown, J. Brown, P. Minnett, W. McKoewn, 1996: Observations of the infrared radiative properties of the ocean - implications for the measurement of sea surface temperature via satellite remote sensing, *Bull. Amer. Meteorol. Soc.*, **77**, 41-51.

Thomas, J.P., R.J. Knight, H.K. Roscoe, J. Turner and C. Symon 1995: An evaluation of a self-calibrating infrared radiometer for measuring sea surface temperature, *J. Atmos. Oceanic Technol.*, **12**, 301-316.

Timofeev, Yu.M. 1966: Thermal sounding of surface water layers by means of thermal radiation, *Izv. Atm. Oceanic Phys.*, 2, 467-469.

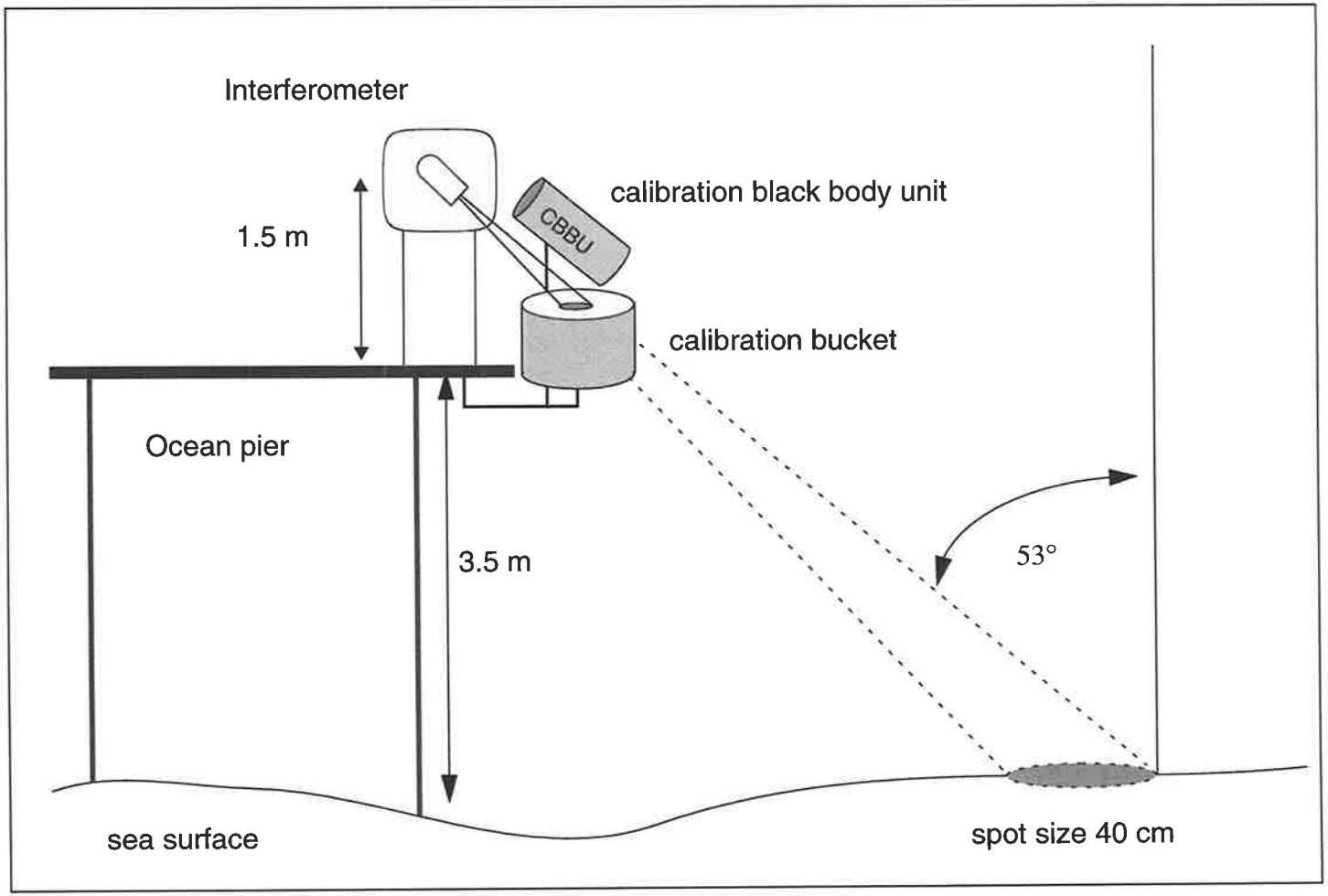

Figure 2: *Sketch of the experimental setup at the head of the ocean pier near Graal-Müritz, Germany, during the measurement period 19-23 October 1995.*

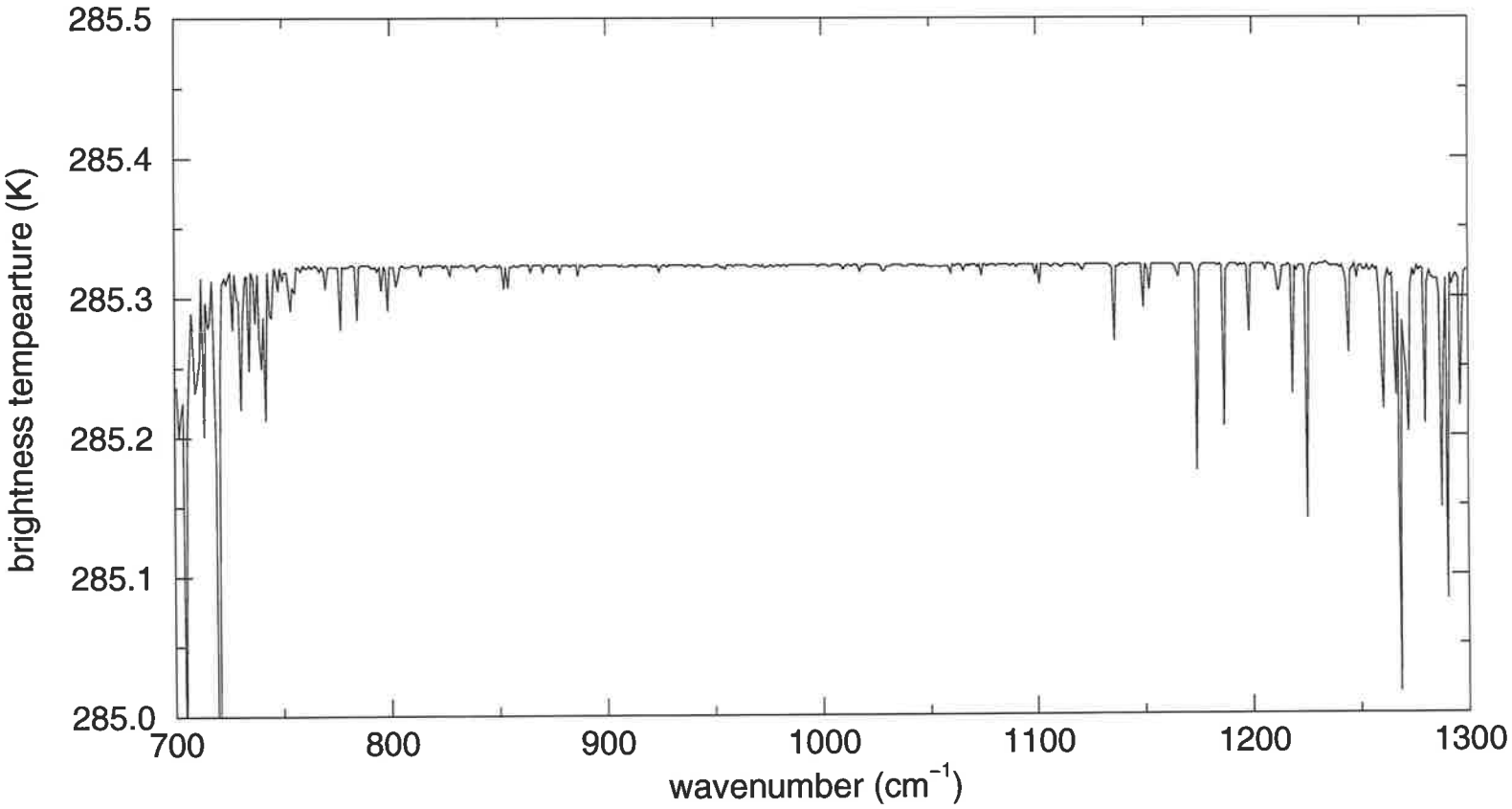

Figure 1: *Spectral brightness temperature for the optical path between sea surface and interferometer during our measurements in October 1995 (see ch. 3 for details) calculated with a line-by-line radiative transfer model.*

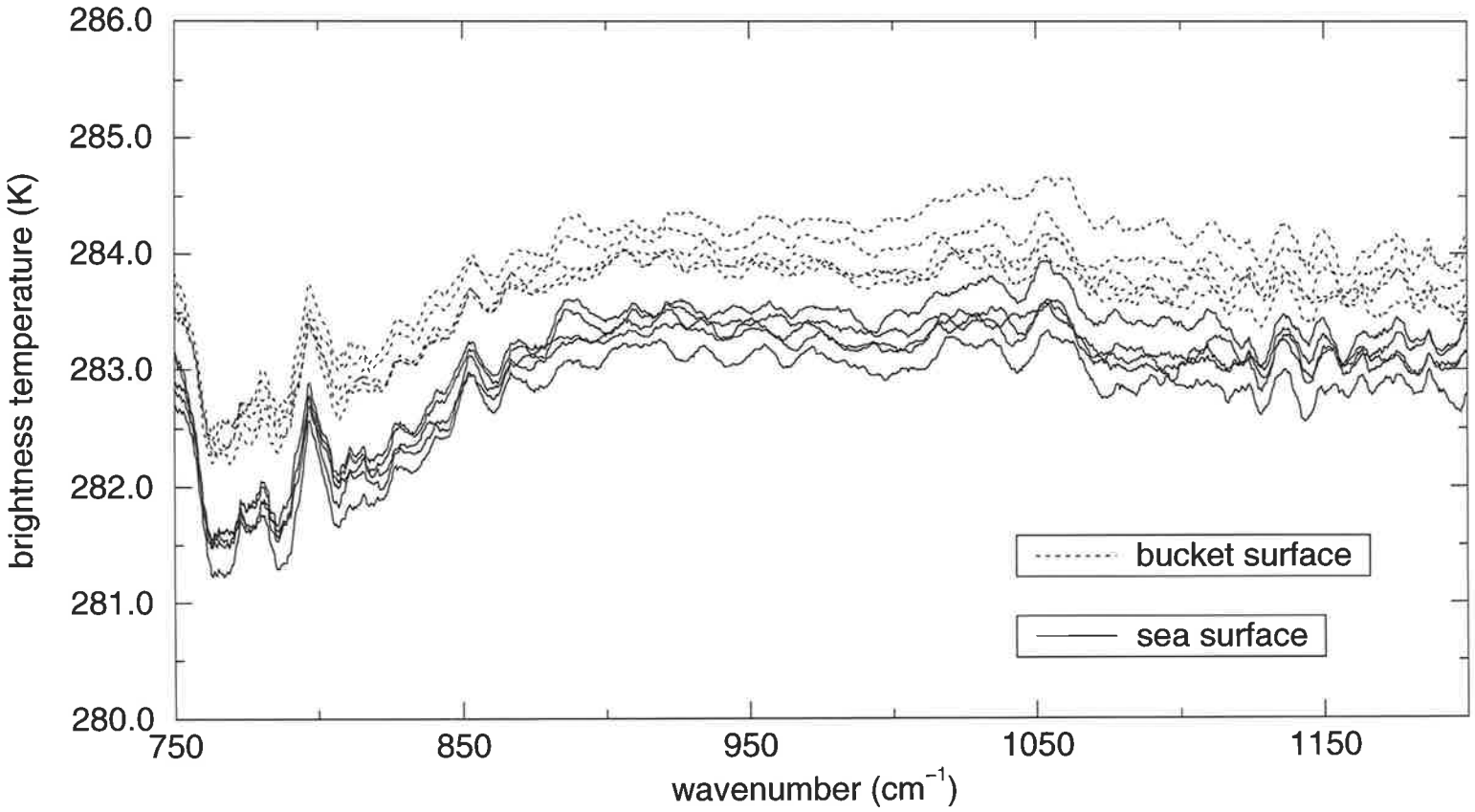

Figure 3: *Calibrated brightness temperature spectra of the sea and the bucket surface. The later is corrected according to the bulk-bucket temperature difference. The spectra are smoothed according to Savitzky and Golay (1964).*

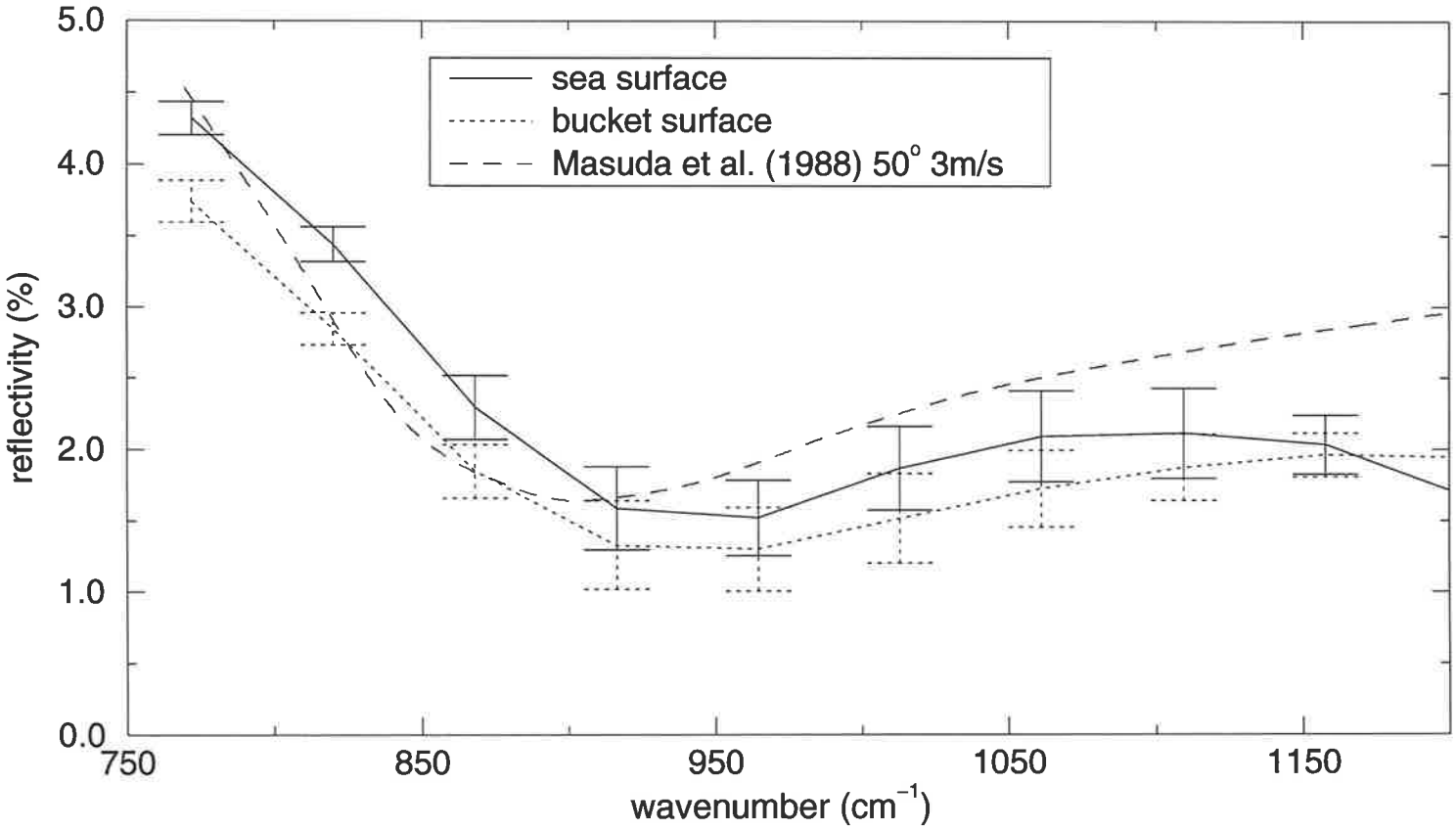

Figure 4: *Spectral reflectivity of the sea and the bucket surface. Theoretical values for 50° view angle and 3m/s wind speed are added from Masuda et al. (1988).*

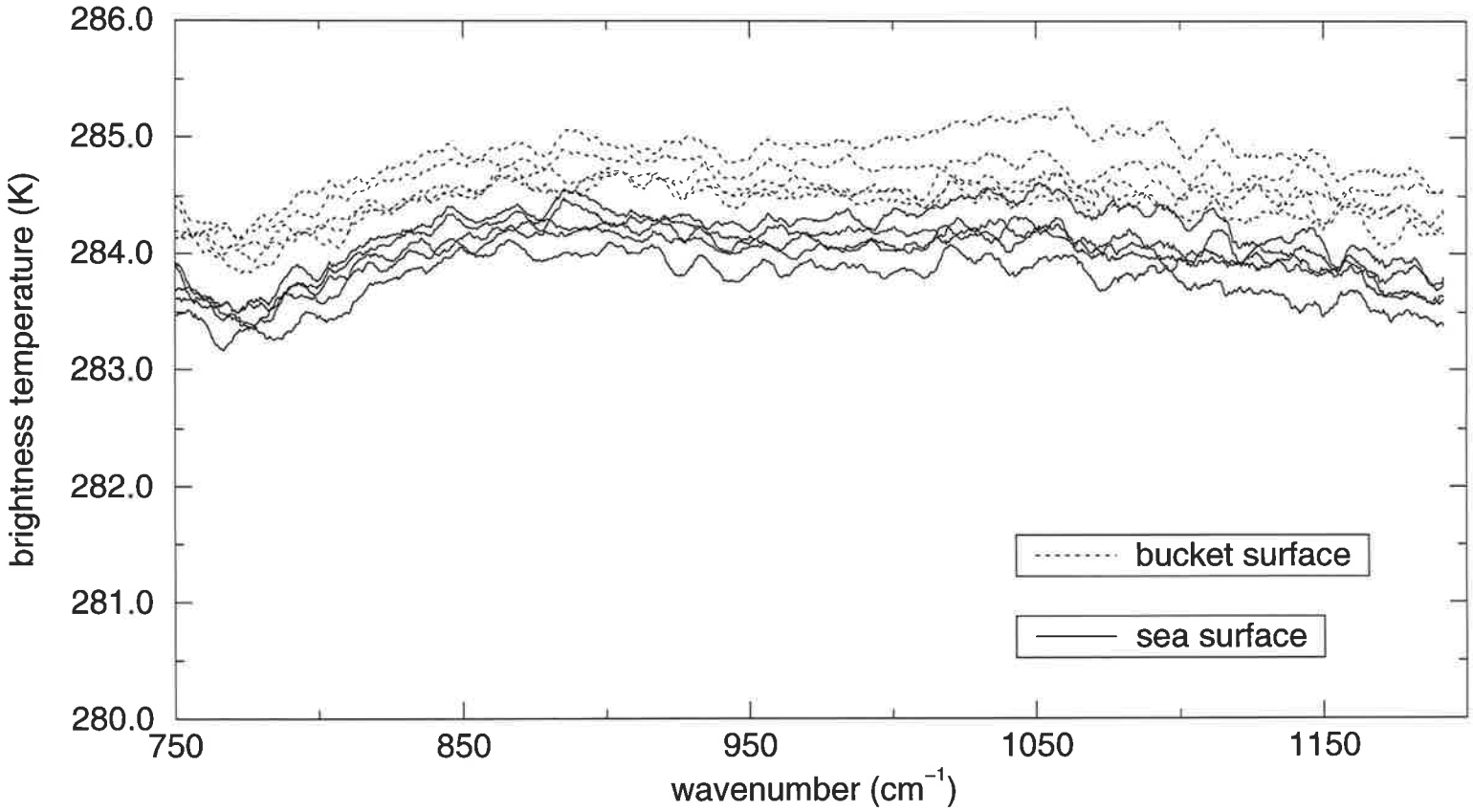

Figure 5: *Sea and bucket surface brightness temperature spectra after correction for the reflected atmospheric component and for emissivity (spectra smoothed as in Fig. 3).*

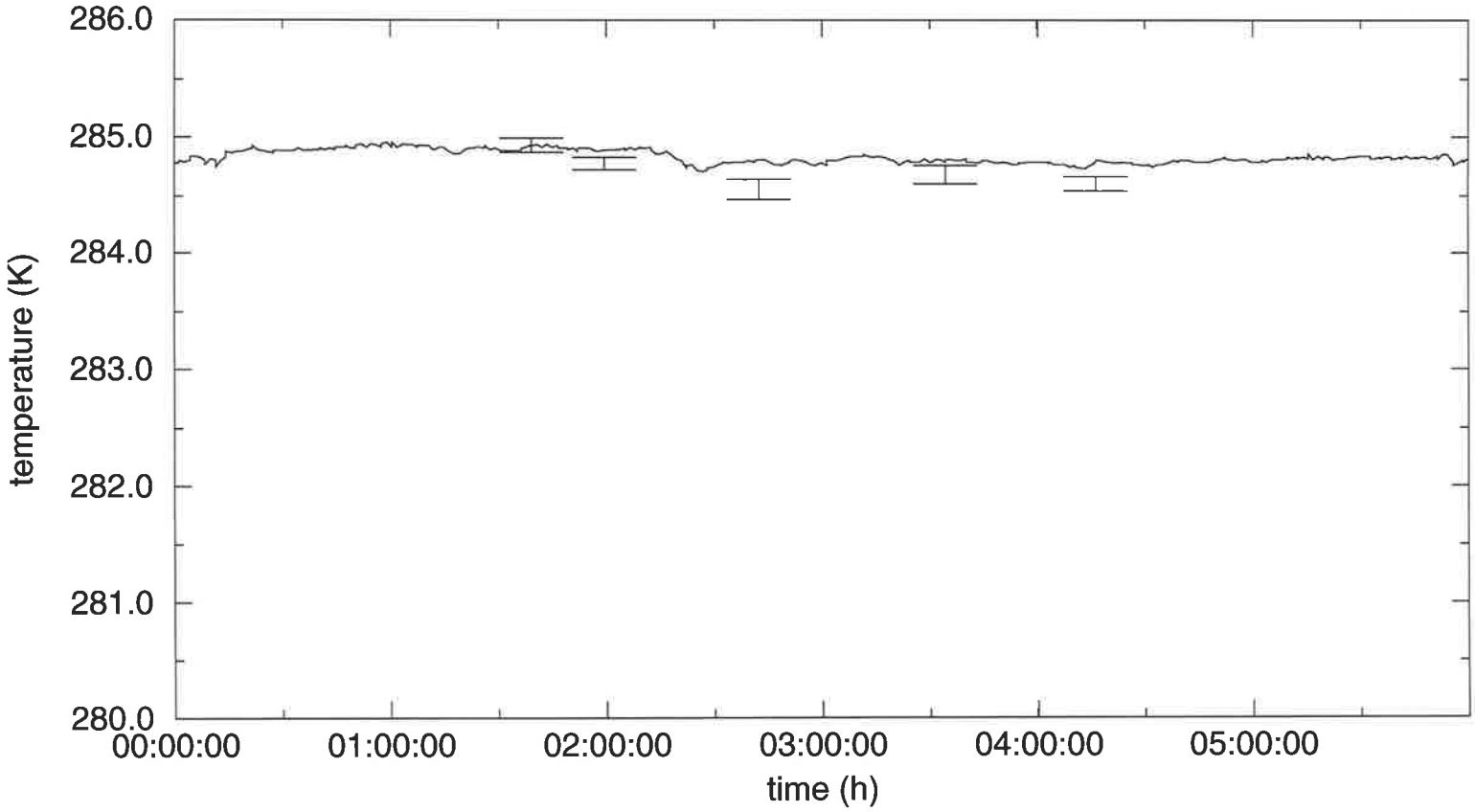

Figure 6: *Comparison between the thermodynamic bucket temperature 1 cm below surface (full line) and spectrally averaged skin temperatures of the bucket at 5 instances calculated with the new multispectral method (bars represent standard deviation of the spectral average between 833 and 1000 cm^{-1})*